Published in final edited form as:
*Nat Neurosci*. 2013 November ; 16(11): 1576–1587. doi:10.1038/nn.3541.

# Non-epithelial stem cells and cortical interneuron production in the human ganglionic eminences

**David V Hansen**[1,2,6], **Jan H Lui**[1,2], **Pierre Flandin**[3,6], **Kazuaki Yoshikawa**[4], **John L Rubenstein**[1,3], **Arturo Alvarez-Buylla**[1,5], and **Arnold R Kriegstein**[1,2]

[1]Eli and Edythe Broad Center of Regeneration Medicine and Stem Cell Research, University of California, San Francisco, San Francisco, California, USA

[2]Department of Neurology, University of California, San Francisco, San Francisco, California, USA

[3]Department of Psychiatry, University of California, San Francisco, San Francisco, California, USA

[4]Laboratory of Regulation of Neuronal Development, Institute for Protein Research, Osaka University, Suita, Osaka, Japan

[5]Department of Neurosurgery, University of California, San Francisco, San Francisco, California, USA

## Abstract

GABAergic cortical interneurons underlie the complexity of neural circuits and are particularly numerous and diverse in humans. In rodents, cortical interneurons originate in the subpallial ganglionic eminences, but their developmental origins in humans are controversial. We characterized the developing human ganglionic eminences and found that the subventricular zone (SVZ) expanded massively during the early second trimester, becoming densely populated with neural stem cells and intermediate progenitor cells. In contrast with the cortex, most stem cells in the ganglionic eminence SVZ did not maintain radial fibers or orientation. The medial ganglionic eminence exhibited unique patterns of progenitor cell organization and clustering, and markers revealed that the caudal ganglionic eminence generated a greater proportion of cortical interneurons in humans than in rodents. On the basis of labeling of newborn neurons in slice culture and mapping of proliferating interneuron progenitors, we conclude that the vast majority of



Correspondence should be addressed to A.R.K. (kriegsteina@stemcell.ucsf.edu), A.A.-B. (abuylla@stemcell.ucsf.edu) or J.L.R. (john.rubenstein@ucsf.edu).
[6]Present addresses: Neuroscience, Genentech, South San Francisco, California, USA (D.V.H.), Quanticel Pharmaceuticals, San Francisco, California, USA (P.F.).

Note: Any Supplementary Information and Source Data files are available in the online version of the paper.

**AUTHOR CONTRIBUTIONS**

D.V.H. and J.H.L. acquired and processed tissue, cultured slices, and performed immunostains, confocal imaging and cell counts. P.F. performed *LHX6 in situ* hybridizations and imaging. K.Y. provided guinea pig antibody to Dlx2. D.V.H. wrote the manuscript. J.L.R., A.A.-B. and A.R.K. provided guidance and conceptual support and edited the manuscript.

**COMPETING FINANCIAL INTERESTS**

The authors declare no competing financial interests.

human cortical interneurons are produced in the ganglionic eminences, including an enormous contribution from non-epithelial SVZ stem cells.

The neurons of the cerebral cortex consist of two broad classes, excitatory and inhibitory. The inhibitory neurons or interneurons (we use the term interneuron in the cortex to refer to GABAergic, inhibitory neurons and it does not include the glutamatergic, spiny stellate neurons of layer IV; the terms cortical and cortex refer to the entire cortical wall, including germinal layers) are GABAergic, form local circuit connections and, in rodents, are generated in subcortical progenitor domains of the ventral telencephalon, primarily in the ganglionic eminences[1]. In humans, cortical interneurons are not only orders of magnitude more numerous than in rodents, but also appear to be more diverse. This raises fundamental questions regarding their origin and migration in the much larger developing human brain that have relevance for understanding interneuron-related disease states, including epilepsy, autism and schizophrenia.

In both the cortex and the ganglionic eminences, newborn neurons derive from neuroepithelial stem cells (radial glia) in the ventricular zone and intermediate progenitors in the SVZ[2,3]. Through asymmetric divisions, radial glia both self-renew and produce neuronal precursors, which can further proliferate before differentiating into neurons. A defined sequence of transcription factors governs the sustained production of neurons from progenitor cells. NOTCH signaling in radial glia activates the expression of HES proteins, which in turn repress proneural transcription factors. In their daughter cells, proneural factors such as ASCL1 (Mash1) direct the expression of NOTCH ligands, which reinforce stem cell maintenance in neighboring radial glia[4]. The combinatorial activities of regionally and temporally specified transcription factors, such as DLX2, NKX2-1 and LHX6 (which are involved in GABAergic neuron production[5–9]), determine the subtype of neuron into which daughter cells will differentiate (Fig. 1a).

The ganglionic eminences consist of three anatomical subdivisions, medial (MGE), lateral (LGE) and caudal (CGE), which are distinguished by molecular markers and the cell types that they produce. The MGE, marked by NKX2-1 expression, gives rise to pallidal projection neurons and to cortical and striatal interneurons[8,10–13]. The LGE is dorsal to the MGE and produces striatal projection neurons, olfactory bulb interneurons and possibly cortical interneurons[13–16]. The CGE, marked by abundant COUP-TFII (NR2F2) expression, includes caudal extensions of the MGE and LGE and generates subtypes of interneurons that are destined for cortex, hippocampus, amygdala and other limbic system nuclei, as well as caudal striatal and pallidal neurons[17–19].

In the mouse, roughly 60–70% of cortical interneurons originate in the MGE, ~30% in the CGE and 5–10% in the preoptic area[1,18,20], suggesting that reported contributions from other regions, such as the LGE and cortex[15,21], are minimal in rodents. In humans, however, it has been proposed that as many as two-thirds of cortical interneurons are produced by cortical progenitors[22], and additional studies have extended on this theme[23–28]. Whether these progenitors originate in the cortex, are ganglionic eminence–derived precursors that continue proliferating after entering the cortex or truly produce cortical interneurons remains uncertain.

We analyzed progenitor cells in the human fetal MGE, LGE and CGE, using nuclear and cytoplasmic markers to distinguish progenitor cell numbers, subtypes and morphologies. The ganglionic eminence SVZ expanded massively during the early second trimester of gestation. We found that a previously unknown type of non-epithelial neural stem cell lacking radial fibers underlies this expansion. We observed unique structural and patterning features of the human MGE, the production of cortical interneurons in the dorsal-most LGE, and a higher proportion of cortical interneurons produced by CGE-type progenitors than in rodent. Slice culture data and analysis of progenitor cell markers did not support the notion that a large proportion of human cortical interneurons are generated in the cortical wall.

## RESULTS

### OSVZ development in the MGE/LGE precedes that in the cortex

To better understand the origins of human cortical interneurons, we examined fetal brain tissues from the late first and early second trimesters (Supplementary Fig. 1), the temporal window during which many cortical neurons are produced, using regional and cell type–specific markers to immunolabel the progenitors of inhibitory neurons (Supplementary Table 1). We observed that the ganglionic eminences expanded markedly in size and cell number between post-conception week 8 (PCW8) and PCW14 (Fig. 1b). Neuroepithelial progenitors diminished over this period, with ventricular zone thickness in the MGE decreasing from an average of 102 ± 6 μm at PCW10 to 58 ± 4 μm at PCW12 ($t_{17}$ = 5.7, $P$ = 0.0001) and 45 ± 4 μm at PCW14 ($t_{14}$ = 7.62, $P$ = 0.00001) (Fig. 1c). Ventricular zone thinning was especially pronounced in the ventromedial MGE, which was reduced to just 25 μm thick by PCW14 (Fig. 1c). Ventricular zone thinning was also observed in the LGE from PCW10 to PCW12 ($t_{15}$ = 4.62, $P$ = 0.002) and PCW14 ($t_{16}$ = 4.69, $P$ = 0.002). In contrast, the SVZ greatly expanded during this interval, becoming densely populated with cells expressing SOX2 and ASCL1 (Fig. 1b,d), with the total MGE reaching a thickness of >2 mm by PCW14, 50-fold greater than the average thickness of the ventricular zone (Fig. 1b,c). These observations suggest that the majority of MGE-derived inhibitory neurons are produced by non-ventricular progenitors in the SVZ.

The overall configuration of proliferative zones in the human and macaque ganglionic eminences (Fig. 1b–d and Supplementary Fig. 2) resembled that described in the developing human and primate cortex[3] and developing mouse ganglionic eminences[29], with three compartments being distinguishable by their cellular components. First, the ventricular zone consisted primarily of cells that express markers of radial glial (neural stem) cells. Second, the inner SVZ (ISVZ, equivalent to the rodent SVZ1)[29] was enriched with cells that express the markers of intermediate progenitors undergoing differentiation to the neuronal lineage (Fig. 1b–d). Third, the outer SVZ (OSVZ) was populated by both of these cell types, in addition to newborn and migrating neurons. The OSVZ is likely related evolutionarily to the rodent SVZ2 (ref. 29), with certain distinctions (Supplementary Fig. 3).

Despite these similarities to cortical germinal regions, SVZ development in the MGE bears two notable differences. First, OSVZ expansion occurred much earlier in the MGE than in cortex. The MGE OSVZ reached a thickness approaching 1 mm by PCW10 (Fig. 1d), whereas the cortical OSVZ had only begun to develop at PCW10 and does not acquire

similar thickness until PCW14 (ref. 30). Second, cell bodies were dispersed in the cortical OSVZ, where much of the volume is occupied with axons and radial glial fibers—features lacking in the MGE OSVZ, where cell density was similar to the degree of packing observed in the ventricular zone and volumetric expansion was exclusively a function of increasing cell numbers.

## The MGE OSVZ is enriched with neural stem cells

Next, we compared the OSVZ progenitor cell composition among the ganglionic eminence domains using markers of progenitor type and proliferation[9,29]. The MGE (marked by intense NKX2-1 staining) and the CGE (marked by intense COUP-TFII staining) expressed SOX2, OLIG2, ASCL1 and Ki67 more densely than the LGE (Fig. 2a). We classified the OSVZ progenitors in each region, using the combinatorial expression of OLIG2, ASCL1 and DLX2 to indicate stages in the progression from undifferentiated radial glia–like cell to committed neuronal precursor (Figs. 1a and 2b,c). Among $OLIG2^+$ cells, those in the MGE were least likely to show signs of differentiation, with just 39.4 ± 2.5% expressing ASCL1 and/or DLX2, versus 71.7 ± 2.1% in the LGE ($t_{25} = 9.89$, $P = 5 \times 10^{-10}$) and 55.2 ± 3.2% in the CGE ($t_{30} = 3.92$, $P = 0.0005$). Among $ASCL1^+$ cells, those in the MGE again appeared less differentiated, with 47.1 ± 3.4% coexpressing DLX2 compared with 71.8 ± 3.4% in the LGE ($t_{25} = 5.18$, $P = 0.00002$) and 66.0 ± 3.4% in the CGE ($t_{30} = 3.95$, $P = 0.0004$). Together, these measurements suggest that progenitor cells in the MGE OSVZ undergo more self-renewing divisions than those in LGE and CGE. The percentage of actively proliferating ($Ki67^+$) OSVZ cells that expressed DLX2 was also lower in the MGE than other ganglionic eminence regions at PCW10 ($t_{16} = 4.39$, $P = 0.0006$, LGE), PCW12 ($t_{23} = 5.66$, $P = 9 \times 10^{-6}$, LGE; $t_{22} = 5.72$, $P = 0.00001$, CGE) and PCW14 ($t_{18} = 7.11$, $P = 0.00001$, LGE), further supporting the idea that MGE progenitors are less differentiated (Fig. 2d).

Further characterization of OSVZ progenitors in the MGE supported the classification of many as neural stem cells. In the mouse MGE, SOX5 is expressed in ventricular radial glia and is downregulated in MGE-derived neurons[31]. In the human MGE, SOX5 expression was not confined to the ventricular zone, but was abundantly present throughout the OSVZ (Fig. 2e), similar to OLIG2. Moreover, most of the $OLIG2^+$ cells in the MGE OSVZ expressed neither NKX2-2 nor SOX10, markers of the oligodendrocyte lineage, suggesting that most $OLIG2^+$ $ASCL1^-$ $DLX2^-$ cells are truly undifferentiated (Fig. 2f). Compared with our measurement that ~40% of $OLIG2^+$ cells in the MGE OSVZ coexpressed ASCL1 and/or DLX2 (Fig. 2c), the scarcity of $OLIG2^+$ $NKX2\text{-}2^+$ cells suggests that the MGE stem cells are primarily devoted to neurogenesis at these ages. In contrast, the sparse $OLIG2^+$ cells in the cortex typically coexpressed NKX2-2 (Fig. 2f), SOX2 and sometimes Ki67 (data not shown), indicating that they are oligodendroglial progenitors. These observations indicate that the human MGE OSVZ supports a large reservoir of undifferentiated $SOX2^+$ $OLIG2^+$ $SOX\ 5^+$ cells that sustains the production of $ASCL1^+$ $DLX2^+$ intermediate progenitors.

## Ganglionic eminence OSVZ stem cells lack radial fibers

Because OSVZ stem cells in both the cortex and ganglionic eminences express radial glial markers, we investigated whether those in the ganglionic eminences exhibit the same

morphology as outer radial glial (oRG) cells in the cortex—unipolar with long radial fibers directed away from the ventricle[3,30]. Using the 4A4 monoclonal antibody to detect phosphorylated vimentin (p-vim) in the cytoplasm of progenitors in M phase, we found that nearly all $4A4^+$ cells in the OSVZ of PCW12 MGE, LGE and CGE appeared as simple, rounded cell bodies, with no emanating fibers, whether they were neuronally committed ($DLX2^+$) or not ($SOX2^+$ $DLX2^-$) (Fig. 3a). This contrasts with cortical OSVZ, where ~40% of all $4A4^+$ cells display oRG cell morphology[30].

The possible distortion of radial fibers by the growth of the basal ganglia raised the concern that any particular tissue section may not have been cut sufficiently parallel to the glial scaffold to observe radial $4A4^+$ fibers. We therefore screened serial frontal (PCW10, 12 and 14), sagittal (PCW10) and horizontal (PCW13) sections, and used nestin staining to visualize radial fibers. Even in sections in which radial fiber orientation was clearly distinguished, nearly all $4A4^+$ OSVZ cells in the MGE, LGE and CGE displayed rounded morphology and no radial fibers. In contrast, we easily identified radial $4A4^+$ fibers in the ventricular zone (Supplementary Fig. 4a), indicating that their scarcity in the OSVZ was unlikely to result simply from sectioning in the wrong plane. In the OSVZ, we observed rare examples of unipolar cells that coexpressed SOX2 and nestin, but their fibers were relatively short, sometimes tortuous, and not usually aligned with $nestin^+$ radial glial fibers (Fig. 3b). Occasionally, $4A4^+$ fibers or cell bodies in the OSVZ were seen to directly contact the microvasculature (Supplementary Fig. 4b). Progenitors with bona fide oRG-type morphology and radial orientation were particularly rare, although we did observe a few examples (Supplementary Fig. 4c–e).

Collectively, these findings indicate that OSVZ stem cells in the ganglionic eminences express markers of radial glia, but do not appear to possess long, radial fibers, which are present in radial glia during all stages of the cell cycle. We surmise that OSVZ progenitors do extend short fibers during interphase that are usually retracted during mitosis. The occasional $4A4^+$ fibers that were observed in the OSVZ suggests that most progenitors are oriented randomly, rather than radially. Other labeling methods with intact tissue will more definitively address whether OSVZ stem cells in the human MGE possess long radial fibers, similar to cortical oRG cells, or have lost epithelial organization.

## Segregation of OSVZ progenitor cells and neurons in the MGE

In the OSVZ of human and primate MGE, we observed two distinct modes of progenitor cell clustering (hereafter referred to as type I and type II). In type I clusters, thin streaks of progenitors extended from the ISVZ into the OSVZ (Fig. 4a and Supplementary Fig. 5a,b). Between these streaks were cells that lacked progenitor markers and expressed *LHX6*, indicating they were postmitotic neurons. At the core of each progenitor streak was a region devoid of nuclei (Fig. 4a). We initially supposed that progenitors might be associated with blood vessels, but staining for collagen, laminin, TIE2, VEGFR2, PECAM1, CD34 and isolectin IB4 disproved this idea (Fig. 4b and data not shown). Instead, the DAPI-negative space was filled with nestin and vimentin, intermediate filament proteins that are expressed by radial glia (Fig. 4b and Supplementary Figs. 4c and 5c). These $nestin^+$ cores were often 7–10 μm in diameter, and some were as thick as 20 μm, whereas individual radial fibers are

~1 μm thick. Thus, type I clusters of MGE progenitors occurred along apparent fascicles of radial glial fibers. A rare 4A4$^+$ cell with oRG morphology and radial orientation (Supplementary Fig. 4c) suggested that certain progenitors associated with these fascicles may migrate to the OSVZ by mitotic somal translocation[30].

Type II MGE progenitor clusters occurred in the OSVZ further from the ventricle and became especially pronounced by PCW14 (Fig. 4c–d and Supplementary Figs. 2 and 6). Broad swaths of progenitor cells clustered between apparent streams of migrating neurons, which expressed DCX and *LHX6*. Unlike type I clusters, type II clusters were not organized around densely bundled glial fibers, as nestin staining was distributed throughout the clusters (Fig. 4c). Neither type I nor type II clustering was apparent in the LGE and CGE, or in rodent MGE (Supplementary Fig. 3).

## Migratory routes and specification of MGE-derived neurons

We immunostained for NKX2-1 and progenitor cell markers to delineate the MGE's borders and identify migratory routes where NKX2-1$^+$ cells exit toward other structures. The MGE is well known for producing GABAergic neurons that migrate tangentially to the cortex[8,13]. Large populations of NKX2-1$^+$ cells with downregulated progenitor markers streamed from the dorsolateral MGE into the LGE (Figs. 1b, 4c and 5a, and Supplementary Fig. 7a). Further into the LGE, NKX2-1 expression dissipated, consistent with findings in rodent that MGE-derived cortical interneurons downregulate NKX2-1 after leaving the MGE[11]. The region in which NKX2-1$^+$ cells invaded the LGE defined a hypo-proliferative span of OSVZ that broadened from PCW10 to PCW14 (Supplementary Fig. 7b), indicative of increasing numbers of MGE-derived neurons migrating into the LGE. Probes for *LHX6* mRNA further revealed MGE-derived cells throughout the entire LGE OSVZ and continuing into the cortex (Fig. 5b), indicating that the LGE is the main corridor for tangentially migrating MGE-derived cortical interneurons.

We also observed NKX2-1$^+$ cells with downregulated progenitor markers moving into the caudate (Supplementary Fig. 7c) and sparsely populating the developing striatum (Fig. 5a), supporting findings in rodent that the MGE generates striatal interneurons[11]. *LHX6*-expressing cells showed a similar striatal distribution (Fig. 5b).

Finally, the MGE also produces projection neurons of the globus pallidus[8,10,12]. In PCW10 sagittal sections, the migration of neurons from the caudoventral aspect of the rostral MGE toward the developing globus pallidus was apparent (Supplementary Fig. 8a), similar to rodents. By PCW12–14, the external (GPe) and internal (GPi) globus pallidi were clearly distinct nuclei, as visualized by NKX2-1 staining (Fig. 5a and Supplementary Fig. 8c). *LHX6* mRNA expression closely matched these findings, showing an apparent stream from the ventral MGE to pallidal structures at PCW10 (Supplementary Fig. 8b) and robust expression in the globus pallidus at PCW14 (Fig. 5b).

Consistent with data from rodent models, these findings indicate that the human MGE produces pallidal projection neurons and cortical and striatal interneurons. The OSVZ appears to be a major source for these MGE-derived cell types, as well as the cellular milieu through which they initially migrate. We also observed transcription factor patterns in the

MGE ventricular zone that are likely to influence the subtypes of interneurons produced in dorsal, ventral and caudal MGE (Supplementary Figs. 9 and 10).

## Increased proportion of CGE-derived cortical interneurons

In the CGE, the ventricular zone could be classified into two domains: the medial side, containing COUP-TFII$^+$ progenitor cells, and the LGE-like lateral side, in which COUP-TFII$^+$ cells were sparser and non-proliferative (Fig. 6a–c and Supplementary Fig. 11). COUP-TFII was also highly expressed in the CGE SVZ (Fig. 6a and Supplementary Figs. 8c, 10b and 11), where it was commonly observed in proliferating (Ki67$^+$) cells (Fig. 6b). In the LGE, COUP-TFII$^+$ DLX2$^+$ cells were abundant throughout its entire SVZ (Fig. 6d and Supplementary Fig. 12a,b), suggesting that many CGE-derived interneurons migrate long distances through the LGE before entering the cortex. COUP-TFII$^+$ cells were uncommon throughout most of MGE (Fig. 6e and Supplementary Figs. 9b and 12b), except in its caudal aspect (Supplementary Fig. 10) and at the interganglionic sulcus (Fig. 6f).

Using COUP-TFII$^+$ cell features to distinguish CGE from LGE revealed stark differences between OSVZ cell populations at the two ends of the CGE-LGE axis, with 74.2 ± 5.0% of CGE cells expressing COUP-TFII compared with 26.5 ± 4.2% of LGE cells (Fig. 6g). Moreover, 31.4 ± 4.7% of the COUP-TFII$^+$ cells in the CGE OSVZ were actively proliferating (Ki67$^+$), whereas this was true for only 3.4 ± 0.7% of LGE COUP-TFII$^+$ cells (without screening for false positives), suggesting that nearly all COUP-TFII$^+$ cells in the LGE were postmitotic, migrating neurons. The vast numbers of CGE- and MGE-derived neurons migrating through the LGE may explain why progenitor markers were less abundant in LGE than in MGE and CGE (Figs. 1d and 2a).

Along the CGE-LGE axis, OSVZ characteristics shifted gradually from CGE-like to LGE-like, suggesting that the CGE and LGE OSVZ is a continuum (Fig. 6g). Supporting a gradual transition from LGE to CGE progenitor cell types, the interganglionic domain of COUP-TFII$^+$ ventricular zone expression (Fig. 6f and Supplementary Fig. 9a,b) was expanded at caudal locations (Supplementary Fig. 10a). This implies that OSVZ progenitor cell composition in a particular location reflects the nearby ventricular zone regions from which the progenitors originated.

To estimate the CGE's contribution to cortical interneuron production, we quantified how frequently cortical DLX2$^+$ cells coexpressed COUP-TFII at different ages and in different regions. COUP-TFII$^+$ DLX2$^-$ cells were not considered, as progenitors and excitatory neurons in some cortical areas expressed COUP-TFII, as did pericytes. Our counts included almost all cortical interneurons, as DLX2$^+$ cells accounted for 96.7 ± 0.8% of cortical cells labeled by a pan-DLX antibody (labeling all inhibitory neurons; data not shown). The fraction of COUP-TFII$^+$ interneurons increased in the cortical SVZ and intermediate zone from 0.34 at PCW10 to 0.54 at PCW14 (Supplementary Fig. 12c). The fraction of COUP-TFII$^+$ interneurons in the cortical plate was approximately half of that in the SVZ and intermediate zone, but increased similarly over this period. These trends are consistent with the developmental expansion of the CGE OSVZ during this period and with the role of the cortical SVZ as a migratory corridor for interneuron precursors.

We estimate that half or more of human cortical interneurons are derived from the CGE, based on the SVZ and intermediate zone numbers, as the vast majority of interneuron precursors were still in the SVZ and intermediate zone at these ages. From our unbiased counts of 2,008 cortical DLX2$^+$ COUP-TFII$^+$ cells, only one was Ki67$^+$ (discussed below), indicating that virtually all CGE-derived interneurons in the cortex at these ages were postmitotic.

## The dorsal LGE, a source of cortical interneurons

We examined the human LGE for patterns of transcription factor expression and evidence of cortical interneuron production. The transcription factor PAX6, known for its expression in cortical radial glia, is also expressed at low levels in the LGE[7,9]. We similarly observed low PAX6 levels in the human LGE (Fig. 7a,b). However, in the dorsal LGE (dLGE) adjacent to the cortex, PAX6 was expressed at high levels, often in conjunction with DLX2$^+$, in ventricular zone and OSVZ progenitor cells (Fig. 7). In mouse, the dLGE produces neurons that migrate via the lateral cortical stream (LCS) to the lateral cortex[32] and some dorsal cortical interneurons[15]. Evidence in PCW12 human tissue supported these findings, with many PAX6$^+$ DLX2$^+$ cells being present in the LCS and lateral cortex (Fig. 7b). We also observed PAX6$^+$ DLX2$^+$ cells in the dorsal cortex up to about a millimeter beyond the dLGE, but not at more dorsal locations (Fig. 7b), implying that infiltration of the dorsal cortex by these cells is very limited unless they downregulate PAX6. The dorsal boundary of the dLGE was sharply defined in the OSVZ, with high levels of DLX2 in progenitor cells, together with Ki67, PAX6, OLIG2, ASCL1 and SOX2 (Fig. 7c,d and Supplementary Fig. 13). In contrast, DLX2 in the cortex was expressed only in the postmitotic interneuron population and at comparatively low levels. The exact location of the boundary in relation to the corticostriatal sulcus varied slightly among tissue samples.

It has been reported that the mouse dLGE also generates COUP-TFII$^+$ cortical interneurons[33]. Our analysis of human tissue did not support this finding, as COUP-TFII$^+$ cells in the dLGE, while abundant, were non-proliferative, presumably CGE-derived interneurons migrating to the cortex (Supplementary Figs. 12b and 13a). Our evidence supports the notion that the dLGE produces certain cortical interneurons, but from PAX6$^+$ rather than COUP-TFII$^+$ progenitors. More selective markers for LGE progenitors and their derivatives will be needed to address whether other LGE regions besides the dLGE produce interneurons destined for the cortex.

## Lack of interneuron production in the cortical wall

We sought to verify reports that a large proportion of human and primate cortical interneurons are generated in the cortex itself at times concurrent with excitatory neurogenesis[22,24]. Because progenitors undergoing commitment to the interneuron lineage express DLX2, we looked extensively for DLX2$^+$ Ki67$^+$ cells in cortical tissues from PCW10–14, examining all layers of the cortical wall in lateral and medial aspects of both dorsal and ventral cortices. Our unbiased searches examined a total of 101 fields containing 6,069 DLX2$^+$ cells, among which only one cell was Ki67$^+$. This cell was within 0.5 mm of the CGE and coexpressed COUP-TFII, suggesting that it was a CGE-derived progenitor cell that moved into the cortex (Supplementary Fig. 14a). To further confirm this conclusion, we

deliberately searched cortical areas for $DLX2^+$ cells coexpressing progenitor markers and found isolated examples (Supplementary Fig. 14b,c); most were within 200 μm of the LGE and CGE and all were within 1 mm, except for some $DLX2^+$ $Ki67^+$ cells in the LCS (Fig. 7b and data not shown). Thus, the few $DLX2^+$ progenitors observed in cortex probably originated in the LGE and CGE, as they were located just outside of those structures. Furthermore, we examined the proliferative state of calretinin $(CALB2)^+$ interneurons in the cortex. Of 766 $DLX2^+$ $CALB2^+$ cells analyzed in nine fields, only one expressed Ki67, and it was also within 0.5 mm of the CGE (Supplementary Fig. 15). These findings suggest that virtually all cortical $DLX2^+$ and $CALB2^+$ inhibitory neuron precursors at these ages are non-proliferative, consistent with evidence in rodents[34].

To address reports that cortical production of interneurons occurs during midgestational ages circa PCW18 (refs. 23,26,28), we cultured slices of PCW18.5 human cortical tissue in the presence of BrdU for 8 d, followed by co-staining for DLX2 and BrdU. We imaged 41 fields containing 3,542 $DLX2^+$ cells and 5,684 $BrdU^+$ cells, among which only 16 were double-labeled (Fig. 8a). Because neurogenesis is abating by this age and gliogenesis is increasing, we also tested younger ages at the peak of cortical neuron production. Slices of PCW15.5 cortex showed a similarly low frequency of DLX2 expression in $BrdU^+$ cells (27 of 3,426) after an 8-d culture period (Fig. 8a). In comparison, 1,159 of 3,443 $BrdU^+$ cells expressed TBR2, a transient progenitor marker for excitatory neuron specification. The culture was permissive for neuronal differentiation, as 10.9% of $BrdU^+$ cells were labeled by antibody to NeuN.

Finally, we sought to quantify interneuron production in whole hemisphere slice cultures. We acquired a rare, large fragment of PCW14.5 brain, which allowed us to test for $DLX2^+$ cell production in dorsal cortex using the ganglionic eminences as a positive control in slices cultured for 8–14 d. Most of the cortical wall contained extremely low numbers of $BrdU^+$ $DLX2^+$ cells, except within ~1 mm of the LGE, which is suggestive of limited tangential migration of interneurons (possibly dLGE-derived) into cortex. Either the culture conditions failed to support more extensive migration or the time in culture was insufficient for newly labeled MGE cells to differentiate and migrate the considerable distance to the cortex. However, this allowed regional analysis of cell type production without the complication of tangential migration from other regions. The difference in $DLX2^+$ cell production between ganglionic eminences and cortex was stark, with as many as 60% of $BrdU^+$ cells in ganglionic eminence fields expressing DLX2, as compared with 0.4, 0.3 and 0.2% in combined cortical fields from >1 mm beyond LGE in 8-, 11- and 14-d slice cultures, respectively (Fig. 8b). Together, our analyses in fixed sections and slice cultures do not support previous reports that a large portion, much less a sizable majority, of human and primate cortical interneurons is produced in the cortex, particularly during the period of peak neurogenesis in the early second trimester.

## DISCUSSION

### Non-epithelial stem cells in the human ganglionic eminences

Our results describe the basic organization and distinguishing features of neural progenitor cells in the human MGE, LGE and CGE. The periventricular compartment was layered,

consisting primarily of radial glia (neural stem cells) in the ventricular zone and their derived intermediate progenitors in the ISVZ. The outer compartment or OSVZ included both stem and intermediate progenitor cells, mixed heterogeneously with newborn and migrating neurons. OSVZ stem cells expressed the same regional fate markers as the ventricular zone radial glia from which they likely originated. The OSVZ progenitor population in the ganglionic eminences expanded markedly in the early second trimester, progressively dwarfing the ventricular zone population.

Unlike the oRG in the cortical OSVZ, putative stem cells in the ganglionic eminence OSVZ appeared to maintain neither a long basal fiber nor radial orientation. The absence of radial fibers on OSVZ stem cells in the human ganglionic eminences prompts the question of why stem cells in the cortical OSVZ maintain fibers. The critical functions of oRG cell fibers in the cortex may have less to do with expanding progenitor numbers and more to do with cell migration, providing a structural foundation for the radial assembly of neurons into discrete columnar units that form the basis of cortical circuitry. Not only are radial fibers unnecessary in the ganglionic eminence OSVZ, as the predominant form of neuronal migration is tangential, but their absence may be vital for packing into a constrained volume the vast numbers of progenitor cells needed to supply the expanding cortex with sufficient numbers of inhibitory neurons.

In the MGE, OSVZ progenitors and neurons uniquely segregated into distinct clusters. In type I clusters, progenitor cells congregated along thick bundles of radial glial fibers that extended from the ventricular zone into the OSVZ. This consolidation of radial fibers may ‘clear the forest’ and facilitate the egress of interneurons from the MGE. The bundles may also function as footholds for OSVZ progenitors, which lack radial fibers, to hold their position against the steady current of tangentially migrating neurons. Type II clusters occur further from the ventricle as OSVZ progenitors and neurons segregate into elongated throngs. These may result as neurons form migratory streams along a path of least resistance where progenitor cells have already been pushed aside, or they may involve self-association of progenitors as in type I clusters.

By PCW14, the percentage of putative interneurons in the cortical SVZ and intermediate zone that expressed COUP-TFII exceeded 50%. This figure may be even higher at later ages, assuming interneuron production in the CGE outlasts the MGE in human as it does in mouse[18]. Thus, more than half of human cortical interneurons likely originate from CGE-type progenitors. Compared with the ~30% in rodent cortex, this increased proportion may reflect the evolutionary expansion in the human and primate lineage of the later-born upper layers of the neocortex, which are preferentially populated with later-born CGE-derived interneurons[18].

## A ventral origin for most human cortical interneurons

We searched extensively for signs of interneuron production by cortical progenitors, but found little evidence to support that it occurs at meaningful levels. In the interneuron lineage, DLX2 expression begins during the progenitor cell stage, but virtually none of the cortical DLX2$^+$ cells that we examined coexpressed Ki67. Isolated exceptions were observed in the SVZ near the LGE and CGE, suggesting a subcortical origin. We also

observed DLX2$^+$ Ki67$^+$ cells in the LCS, indicating that certain migratory LGE-derived cells proliferate outside their primary germinal region, as previously observed among cells destined for the olfactory bulb in the rostral migratory stream[35].

We also attempted, with little success, to validate reports that inhibitory neuron production can be observed in cultured slices of cortical tissue or in cultures of dissociated cortical progenitors[22,26]. Our previous efforts with dissociated progenitors from PCW13.5 cortex yielded only neurons of the excitatory lineage[30]. In slices from PCW14.5–18.5 tissues, after 8–14 d in culture, we found that the portion of cortical BrdU$^+$ cells that expressed DLX2 was consistently <1%. Thus, proliferation of interneuron precursors in cortex is possibly present, but extremely limited compared with other progenitor cell activities.

Small numbers of mouse cortical interneurons are produced post-natally in the cortical SVZ, when excitatory neuron production is complete[21,36,37]. These interneuron precursors could be equivalent to the infrequent DLX2$^+$ BrdU$^+$ cells that we observed in human cortical slice cultures. Fate-mapping experiments and the expression of 5-HT$_{3A}$ receptor support a ventral CGE origin for these interneuron precursors in mouse. Nonetheless, the apparent pallial origin of certain olfactory interneurons[38] suggests that some cortical progenitors have the capacity to produce inhibitory neurons. Regardless of origin, most interneurons generated in the postnatal cortical SVZ populate the olfactory bulb, with only a minor fraction staying in cortex[36]—probably reflecting a transitory period during which interneuron migratory behavior shifts from cortical dispersion to chain migration in the rostral migratory stream[39]. Thus, reports of interneuron production in human cortex at midgestation should be interpreted cautiously, as the cells being produced at that stage may migrate to other brain regions.

### Alternative interpretations of historical data

Additional observations have fueled the belief that cortical progenitor cells throughout human and primate evolution have become a well-spring for cortical interneurons[40]. Our interpretations of the data lead us to other conclusions and frequently implicate the CGE rather than the cortex as a likely source for the interneurons in question.

The expression of ASCL1 in approximately two-thirds of DLX2$^+$ cortical interneurons at PCW23 and the observation of ASCL1$^+$ (but not DLX2$^+$) cortical progenitors during the neurogenic period, was interpreted to mean that the ASCL1$^+$ DLX2$^+$ interneurons originated in the cortex, as MGE-derived interneurons downregulate ASCL1 after neuronal commitment[22]. However, three observations suggest a different interpretation. First, cortical progenitors express ASCL1 at much lower levels than ganglionic eminence progenitors and in the same cells that express TBR2 and/or NEUROG2, which are determinants of the excitatory lineage[30] (data not shown). Second, low-level ASCL1 expression is similarly observed in progenitor cells of embryonic mouse cortex[9,41], which do not produce cortical inhibitory neurons. Third, many CGE-derived interneurons in mouse continue to express ASCL1 after they have migrated into the cortex[18]. This provides a simpler explanation for the origin of ASCL1$^+$ DLX2$^+$ human cortical interneurons, as there is no convincing evidence that many cortical interneurons wait until the post-proliferative stage to induce DLX2 expression. Given the increase in CGE-derived cortical interneurons from ~35% at

PCW10 to >50% at PCW14, it would not be surprising to learn that about two-thirds of cortical interneurons were derived from the CGE by PCW23.

The greater abundance and morphological diversity of interneurons in human compared with rodent cortex has further heightened speculation that many human cortical interneurons have a distinct cortical origin. In particular, double bouquet cells are abundant in primate cortex, but (depending on the stringency of criteria[42–44]) are not observed in rodents[45]. However, double bouquet cells share several traits—bitufted, radial orientation, CALB2$^+$ and preferential residence in upper cortical layers—with certain CGE-derived interneurons in rodents that could be their cellular equivalents[17,18,44,46]. Along with observations of double bouquet cells in evolutionarily more distant carnivores[47], this suggests that double bouquets are in an interneuron class that varies among species in degree of axonal elaboration, but has a common location of origin, the CGE.

The brains of human fetuses or infants with holoprosencephaly show pronounced striatal hypoplasia as a result of developmental failure in the ganglionic eminences[48]. The decrease in SST$^+$, NPY$^+$ and NOS$^+$ cortical interneurons, together with the normal abundance of CALB2$^+$ interneurons, has been interpreted to mean that ganglionic eminence–derived interneurons are lost, whereas cortex-derived interneurons are preserved[25,40]. However, in these brains, only the NKX2-1$^+$ germinal region was critically affected, as DLX2 and ASCL1 were expressed normally throughout the extant subpallium. Thus, a simpler explanation is that MGE-derived interneurons were lost, while CGE-derived interneurons were largely unaffected. The known production of CALB2$^+$ interneurons by the CGE[44], and the fact that MGE progenitor cells convert to CGE-type cells and produce CALB2$^+$ interneurons when NKX2-1 expression is lost[49], support our interpretation of the holoprosencephaly data.

Finally, observations of radially oriented interneurons in the primate cortical ventricular zone have been used to argue that the cells are generated locally, as they and excitatory neurons appear to have the same place of origin and use similar modes of migration[24,25]. This argument can be discounted by live imaging that found that ganglionic eminence–derived interneurons in the cortex switch from tangential to radial migration, sometimes descending into the ventricular zone before ascending to the cortical plate[50].

In summary, our data do not support the claim that a majority of human cortical interneurons are produced in the cortex. Although we have not examined tissues beyond the second trimester, our results indicate that the ganglionic eminences are responsible for most cortical interneuron production. The ganglionic eminence OSVZ developed earlier than the cortical OSVZ, expanded to a greater thickness and was more densely packed with progenitor cells. We propose that a huge reservoir of non-epithelial stem cells in the OSVZ of the ganglionic eminences supplies essentially all of the interneurons needed in the cortex. Further research will be required to definitively settle this debate, which has important implications for understanding cortical development, disease and cell therapy.

# ONLINE METHODS

## Tissue collection and processing

Human fetal brain tissue was collected from elective pregnancy termination specimens at San Francisco General Hospital, usually within 2 h of the procedure, except for the PCW10 tissue, which was collected 4 h post-procedure. Donated human tissues were examined only from patients who had previously given informed consent and in strict observance of state and institutional legal and ethical requirements. Research protocols were approved by the Committee on Human Research at University of California, San Francisco. We measured fetal foot length to determine gestational age, and tissues were transported by shuttle, on ice in Leibowitz-15 medium, to the laboratory for further examination and processing. Total post-mortem interval was typically 3–4 h before fixation or 4–5 h before commencing slice culture. For cryosections, tissues were fixed in 4% paraformaldehyde (wt/vol) in phosphatebuffered saline (PBS) at 4 °C for at least 3 d, dehydrated in 30% sucrose (wt/vol) in PBS at 4 °C, embedded and frozen at −80 °C in O.C.T. compound (Tissue-Tek), and sectioned on a Leica CM3050S (16–30 μm thick) onto glass slides, which were stored at −80 °C. For macaque tissue, paraformaldehyde-fixed fetal brains were purchased from the California National Primate Research Center, The brains were placed in fixative immediately following tissue harvest and dissection, with a post-mortem interval of less than 1 h, followed by transport to our laboratory for further processing.

For cortical slice cultures, tissue was embedded in 4% low melting point agarose in artificial cerebrospinal fluid (ACSF; 125 mM NaCl, 2.5 mM KCl, 1 mM $MgCl_2$, 2 mM $CaCl_2$, 1.25 mM $NaH_2PO_4$, 25 mM $NaHCO_3$, 25 mM D-(+)-glucose, bubbled with 95% $O_2$/5% $CO_2$), sliced in ice-chilled ACSF using a Leica VT1200S vibratome (300 μm thick), transferred and suspended on Millicell-CM slice culture inserts (Millipore), and cultured for 8–14 d at 37 °C in 5% $CO_2$, 8% $O_2$, balance $N_2$ in the presence of 15 μg $ml^{-1}$ BrdU (Sigma), diluted in slice culture medium: 66% Eagle's Basal Medium, 25% Hanks-buffered saline solution, 5% fetal bovine serum, 1% N-2 supplement (Invitrogen), 0.66% D-(+)-glucose, penicillin-streptomycin-glutamine (Invitrogen). Slices were paraformaldehyde-fixed overnight and stored at 4 °C in PBS plus 0.1% sodium azide (wt/vol).

## Immunohistochemistry

Cryosections were thawed in PBS, immersed in nearly boiling 0.01 M sodium citrate (pH 6.0) for 10 min for antigen retrieval, returned to PBS and then incubated for 1 h at 21 °C in blocking buffer (PBS plus 0.1% Triton X-100 (by volume), 5–10% donkey or goat normal serum (vol/vol), and 0.2% gelatin or bovine serum albumin (wt/vol)). Primary and secondary antibodies were diluted in blocking buffer. Sections were incubated with primary antibodies for 3 h at 21 °C or overnight at 4 °C. Primary stains were washed in PBS plus 0.1% Triton X-100 with three changes of wash buffer for a total of at least 2 h washing. Sections were incubated with secondary antibodies and DAPI (4′,6-diamidino-2-phenylindole) for 60–90 min at 21 °C, and secondary stains were washed as described above. Cover slips were mounted using Aqua-Poly/Mount (Polysciences) and air dried at 21 °C overnight in the dark. Cultured, BrdU-labeled slices were fixed and stained as described previously[30].

All primary antibodies used in this study are listed in Supplementary Table 1. The development of guinea pig antibody to DLX2 (ref. 51) and rabbit antibody to dll (pan-DLX)[52] were described previously. Secondary antibodies used included goat antibodies to rabbit, mouse and guinea pig IgG, goat antibodies to mouse IgG1 or IgG2a, donkey antibodies to mouse, rabbit, rat or goat IgG, conjugated to Alexa Fluor 488, 546, 594 or 647 (Invitrogen A11073, A11030, A21245, A21121, A21123, A21240, A21131, A21241, A21202, A10036, A31571, A21206, A21207, A10040, A31573, A11055, A11056, A21447, A21208), and donkey antibody to guinea pig IgG or chicken IgY conjugated to Cy3 (Millipore AP194C, AP193C). Alexa Fluor 488 conjugates were diluted 1:1,000 and all others were used at 1:500.

### Confocal imaging, image processing and quantifications

All images were acquired on Leica TCS SP5 laser confocal microscopes. For subregional views of tissue sections using specific markers, images were acquired in Tilescan mode with automatic stitching of arrayed tiles using either 10× lens with 1.5–2.0× optical zoom or else 20× lens with 1.0× optical zoom, and confocal *z* stacks of optical sections were displayed as maximum intensity projections. For DAPI-only views of entire tissue sections, Tilescan images were acquired using a 5× lens. For all cell-counting analyses and close-up images of progenitor cells (for example, *z* stack projections for $4A4^+$ cells), images were acquired using 63× oil immersion lens, sometimes with additional optical zoom. Confocally imaged data files were opened using Imaris imaging software (Bitplane) for colocalization analyses or other quantifications and for generation of TIFF files. Adjustments to image brightness and contrast for publication figures were performed using Adobe Photoshop, and line art was added using Adobe Illustrator.

Colocalization counts were performed as described previously[30]. For the counts shown in Figure 2c,d, two or more well-spaced OSVZ images were acquired per ganglionic eminence region per section from at least three frontal sections spaced along rostral-caudal extent of the tissues. For the counts in Figure 6g, at least three well-spaced OSVZ images were acquired per position along the CGE-LGE axis, with paired positions 1 and 6, 2 and 5, or 3 and 4 coming from the same slide, and positions 1–3 coming from the inferior CGE/LGE and positions 4–6 from the superior LGE/CGE on those slides. For cortical cell counts of DLX2, Ki67 and COUP-TFII coexpression, multiple images for each layer of the cortical wall were acquired from lateral, intermediate and medial regions of dorsal cortex (PCW10, 12 and 14) or ventral cortex (PCW12 only) from frontal sections spaced along the rostral-caudal axis, and from a PCW10 sagittal section. For BrdU cell counts in cultured slices, images were acquired mainly from germinal regions but other areas were also screened to ensure a complete analysis. For quantifying average ventricular zone thickness, measurements were taken from ventral and dorsal regions of both MGE and LGE, from multiple frontal sections at different rostral-caudal locations. All error bars in graphs represent s.e.m. for single tissue samples, with data gathered from multiple sections per tissue sample and multiple fields per section. Statistical comparisons between sample populations were performed using the *t* test function in Excel (unpaired, two-tailed, unequal variance). Cell counts using pan-DLX antibody or calretinin antibody were each obtained using a single frontal section of PCW12 tissue, with multiple fields from both dorsal and

ventral cortex used for colocalization analyses. Raw numbers for ventricular zone measurements and all cell count/colocalization studies are available in spreadsheet format in the Source Data.

### *In situ* hybridizations for *LHX6* mRNA and imaging

Human *LHX6* coding sequence was obtained from Open Biosystems and subcloned into pCS2+$HA_3$ plasmid. Linearized plasmid was transcribed *in vitro* using T7 promoter and DIG-labeled antisense probe was hybridized to paraformaldehyde-fixed cryosections as described previously[53].

## Supplementary Material

Refer to Web version on PubMed Central for supplementary material.

## Acknowledgments

We thank the staff at San Francisco General Hospital Women's Options Center for their consideration in allowing access to donated human fetal tissue. We thank S. Davis and co-workers at the California National Primate Research Center for providing fixed brain tissue from fetal macaques. We also thank W. Walantus, K. Wang, S. Wang, Y. Wang and other University of California at San Francisco personnel for technical and administrative support. We are very grateful to J. Kohtz (Northwestern University) for sharing her final aliquot of pan-Dlx antibody. The NKX2-2 antibody developed by T. Jessell and S. Brenner-Morton was obtained from the Developmental Studies Hybridoma Bank, developed under the auspices of the National Institute of Child Health and Human Development and maintained by the University of Iowa Department of Biology. This work was supported by grants from the National Institute of Neurological Disorders and Stroke and the National Institute of Mental Health of the US National Institutes of Health, California Institute for Regenerative Medicine, John G. Bowes Research Fund and from Bernard Osher.

## References

1. Wonders CP, Anderson SA. The origin and specification of cortical interneurons. Nat. Rev. Neurosci. 2006; 7:687–696. [PubMed: 16883309]
2. Brown KN, et al. Clonal production and organization of inhibitory interneurons in the neocortex. Science. 2011; 334:480–486. [PubMed: 22034427]
3. Lui JH, Hansen DV, Kriegstein AR. Development and evolution of the human neocortex. Cell. 2011; 146:18–36. [PubMed: 21729779]
4. Kageyama R, Ohtsuka T, Hatakeyama J, Ohsawa R. Roles of bHLH genes in neural stem cell differentiation. Exp. Cell Res. 2005; 306:343–348. [PubMed: 15925590]
5. Alifragis P, Liapi A, Parnavelas JG. Lhx6 regulates the migration of cortical interneurons from the ventral telencephalon but does not specify their GABA phenotype. J. Neurosci. 2004; 24:5643–5648. [PubMed: 15201337]
6. Anderson SA, Eisenstat DD, Shi L, Rubenstein JL. Interneuron migration from basal forebrain to neocortex: dependence on Dlx genes. Science. 1997; 278:474–476. [PubMed: 9334308]
7. Flames N, et al. Delineation of multiple subpallial progenitor domains by the combinatorial expression of transcriptional codes. J. Neurosci. 2007; 27:9682–9695. [PubMed: 17804629]
8. Sussel L, Marin O, Kimura S, Rubenstein JL. Loss of Nkx2.1 homeobox gene function results in a ventral to dorsal molecular respecification within the basal telencephalon: evidence for a transformation of the pallidum into the striatum. Development. 1999; 126:3359–3370. [PubMed: 10393115]
9. Yun K, et al. Modulation of the notch signaling by Mash1 and Dlx1/2 regulates sequential specification and differentiation of progenitor cell types in the subcortical telencephalon. Development. 2002; 129:5029–5040. [PubMed: 12397111]

10. Flandin P, Kimura S, Rubenstein JL. The progenitor zone of the ventral medial ganglionic eminence requires Nkx2-1 to generate most of the globus pallidus but few neocortical interneurons. J. Neurosci. 2010; 30:2812–2823. [PubMed: 20181579]
11. Marin O, Anderson SA, Rubenstein JL. Origin and molecular specification of striatal interneurons. J. Neurosci. 2000; 20:6063–6076. [PubMed: 10934256]
12. Nobrega-Pereira S, et al. Origin and molecular specification of globus pallidus neurons. J. Neurosci. 2010; 30:2824–2834. [PubMed: 20181580]
13. Wichterle H, Turnbull DH, Nery S, Fishell G, Alvarez-Buylla A. *In utero* fate mapping reveals distinct migratory pathways and fates of neurons born in the mammalian basal forebrain. Development. 2001; 128:3759–3771. [PubMed: 11585802]
14. Deacon TW, Pakzaban P, Isacson O. The lateral ganglionic eminence is the origin of cells committed to striatal phenotypes: neural transplantation and developmental evidence. Brain Res. 1994; 668:211–219. [PubMed: 7704606]
15. Ma T, et al. A subpopulation of dorsal lateral/caudal ganglionic eminence–derived neocortical interneurons expresses the transcription factor sp8. Cereb. Cortex. 2012; 22:2120–2130. [PubMed: 22021915]
16. Olsson M, Campbell K, Wictorin K, Bjorklund A. Projection neurons in fetal striatal transplants are predominantly derived from the lateral ganglionic eminence. Neuroscience. 1995; 69:1169–1182. [PubMed: 8848105]
17. Kanatani S, Yozu M, Tabata H, Nakajima K. COUP-TFII is preferentially expressed in the caudal ganglionic eminence and is involved in the caudal migratory stream. J. Neurosci. 2008; 28:13582–13591. [PubMed: 19074032]
18. Miyoshi G, et al. Genetic fate mapping reveals that the caudal ganglionic eminence produces a large and diverse population of superficial cortical interneurons. J. Neurosci. 2010; 30:1582–1594. [PubMed: 20130169]
19. Nery S, Fishell G, Corbin JG. The caudal ganglionic eminence is a source of distinct cortical and subcortical cell populations. Nat. Neurosci. 2002; 5:1279–1287. [PubMed: 12411960]
20. Gelman D, et al. A wide diversity of cortical GABAergic interneurons derives from the embryonic preoptic area. J. Neurosci. 2011; 31:16570–16580. [PubMed: 22090484]
21. Inta D, et al. Neurogenesis and widespread forebrain migration of distinct GABAergic neurons from the postnatal subventricular zone. Proc. Natl. Acad. Sci. USA. 2008; 105:20994–20999. [PubMed: 19095802]
22. Letinic K, Zoncu R, Rakic P. Origin of GABAergic neurons in the human neocortex. Nature. 2002; 417:645–649. [PubMed: 12050665]
23. Jakovcevski I, Mayer N, Zecevic N. Multiple origins of human neocortical interneurons are supported by distinct expression of transcription factors. Cereb. Cortex. 2011; 21:1771–1782. [PubMed: 21139075]
24. Petanjek Z, Berger B, Esclapez M. Origins of cortical GABAergic neurons in the cynomolgus monkey. Cereb. Cortex. 2009; 19:249–262. [PubMed: 18477686]
25. Petanjek Z, Kostovic I, Esclapez M. Primate-specific origins and migration of cortical GABAergic neurons. Front. Neuroanat. 2009; 3:26. [PubMed: 20011218]
26. Yu X, Zecevic N. Dorsal radial glial cells have the potential to generate cortical interneurons in human but not in mouse brain. J. Neurosci. 2011; 31:2413–2420. [PubMed: 21325508]
27. Zecevic N, Chen Y, Filipovic R. Contributions of cortical subventricular zone to the development of the human cerebral cortex. J. Comp. Neurol. 2005; 491:109–122. [PubMed: 16127688]
28. Zecevic N, Hu F, Jakovcevski I. Interneurons in the developing human neocortex. Dev. Neurobiol. 2011; 71:18–33. [PubMed: 21154907]
29. Petryniak MA, Potter GB, Rowitch DH, Rubenstein JL. Dlx1 and Dlx2 control neuronal versus oligodendroglial cell fate acquisition in the developing forebrain. Neuron. 2007; 55:417–433. [PubMed: 17678855]
30. Hansen DV, Lui JH, Parker PR, Kriegstein AR. Neurogenic radial glia in the outer subventricular zone of human neocortex. Nature. 2010; 464:554–561. [PubMed: 20154730]

31. Azim E, Jabaudon D, Fame RM, Macklis JD. SOX6 controls dorsal progenitor identity and interneuron diversity during neocortical development. Nat. Neurosci. 2009; 12:1238–1247. [PubMed: 19657336]
32. Carney RS, et al. Cell migration along the lateral cortical stream to the developing basal telencephalic limbic system. J. Neurosci. 2006; 26:11562–11574. [PubMed: 17093077]
33. Cai Y, et al. Nuclear receptor COUP-TFII-expressing neocortical interneurons are derived from the medial and lateral/caudal ganglionic eminence and define specific subsets of mature interneurons. J. Comp. Neurol. 2013; 521:479–497. [PubMed: 22791192]
34. Xu Q, de la Cruz E, Anderson SA. Cortical interneuron fate determination: diverse sources for distinct subtypes? Cereb. Cortex. 2003; 13:670–676. [PubMed: 12764043]
35. Menezes JR, Smith CM, Nelson KC, Luskin MB. The division of neuronal progenitor cells during migration in the neonatal mammalian forebrain. Mol. Cell Neurosci. 1995; 6:496–508. [PubMed: 8742267]
36. Wu S, et al. Tangential migration and proliferation of intermediate progenitors of GABAergic neurons in the mouse telencephalon. Development. 2011; 138:2499–2509. [PubMed: 21561989]
37. Riccio O, et al. New pool of cortical interneuron precursors in the early postnatal dorsal white matter. Cereb. Cortex. 2012; 22:86–98. [PubMed: 21616983]
38. Ventura RE, Goldman JE. Dorsal radial glia generate olfactory bulb interneurons in the postnatal murine brain. J. Neurosci. 2007; 27:4297–4302. [PubMed: 17442813]
39. Battista D, Rutishauser U. Removal of polysialic acid triggers dispersion of subventricularly derived neuroblasts into surrounding CNS tissues. J. Neurosci. 2010; 30:3995–4003. [PubMed: 20237270]
40. Jones EG. The origins of cortical interneurons: mouse versus monkey and human. Cereb. Cortex. 2009; 19:1953–1956. [PubMed: 19429862]
41. Guillemot F, Joyner AL. Dynamic expression of the murine Achaete-Scute homologue Mash-1 in the developing nervous system. Mech. Dev. 1993; 42:171–185. [PubMed: 8217843]
42. Connor JR, Peters A. Vasoactive intestinal polypeptide–immunoreactive neurons in rat visual cortex. Neuroscience. 1984; 12:1027–1044. [PubMed: 6384816]
43. Kawaguchi Y, Kubota Y. Physiological and morphological identification of somatostatin- or vasoactive intestinal polypeptide–containing cells among GABAergic cell subtypes in rat frontal cortex. J. Neurosci. 1996; 16:2701–2715. [PubMed: 8786446]
44. Butt SJ, et al. The temporal and spatial origins of cortical interneurons predict their physiological subtype. Neuron. 2005; 48:591–604. [PubMed: 16301176]
45. Feldman ML, Peters A. The forms of non-pyramidal neurons in the visual cortex of the rat. J. Comp. Neurol. 1978; 179:761–793. [PubMed: 346619]
46. del Rio MR, DeFelipe J. Double bouquet cell axons in the human temporal neocortex: relationship to bundles of myelinated axons and colocalization of calretinin and calbindin D-28k immunoreactivities. J. Chem. Neuroanat. 1997; 13:243–251. [PubMed: 9412906]
47. Somogyi P, Cowey A. Combined Golgi and electron microscopic study on the synapses formed by double bouquet cells in the visual cortex of the cat and monkey. J. Comp. Neurol. 1981; 195:547–566. [PubMed: 7462443]
48. Fertuzinhos S, et al. Selective depletion of molecularly defined cortical interneurons in human holoprosencephaly with severe striatal hypoplasia. Cereb. Cortex. 2009; 19:2196–2207. [PubMed: 19234067]
49. Xu Q, et al. Sonic hedgehog signaling confers ventral telencephalic progenitors with distinct cortical interneuron fates. Neuron. 2010; 65:328–340. [PubMed: 20159447]
50. Nadarajah B, Alifragis P, Wong RO, Parnavelas JG. Ventricle-directed migration in the developing cerebral cortex. Nat. Neurosci. 2002; 5:218–224. [PubMed: 11850632]
51. Kuwajima T, Nishimura I, Yoshikawa K. Necdin promotes GABAergic neuron differentiation in cooperation with Dlx homeodomain proteins. J. Neurosci. 2006; 26:5383–5392. [PubMed: 16707790]
52. Kohtz JD, et al. N-terminal fatty-acylation of sonic hedgehog enhances the induction of rodent ventral forebrain neurons. Development. 2001; 128:2351–2363. [PubMed: 11493554]

53. Jeong J, et al. Dlx genes pattern mammalian jaw primordium by regulating both lower jaw-specific and upper jaw-specific genetic programs. Development. 2008; 135:2905–2916. [PubMed: 18697905]

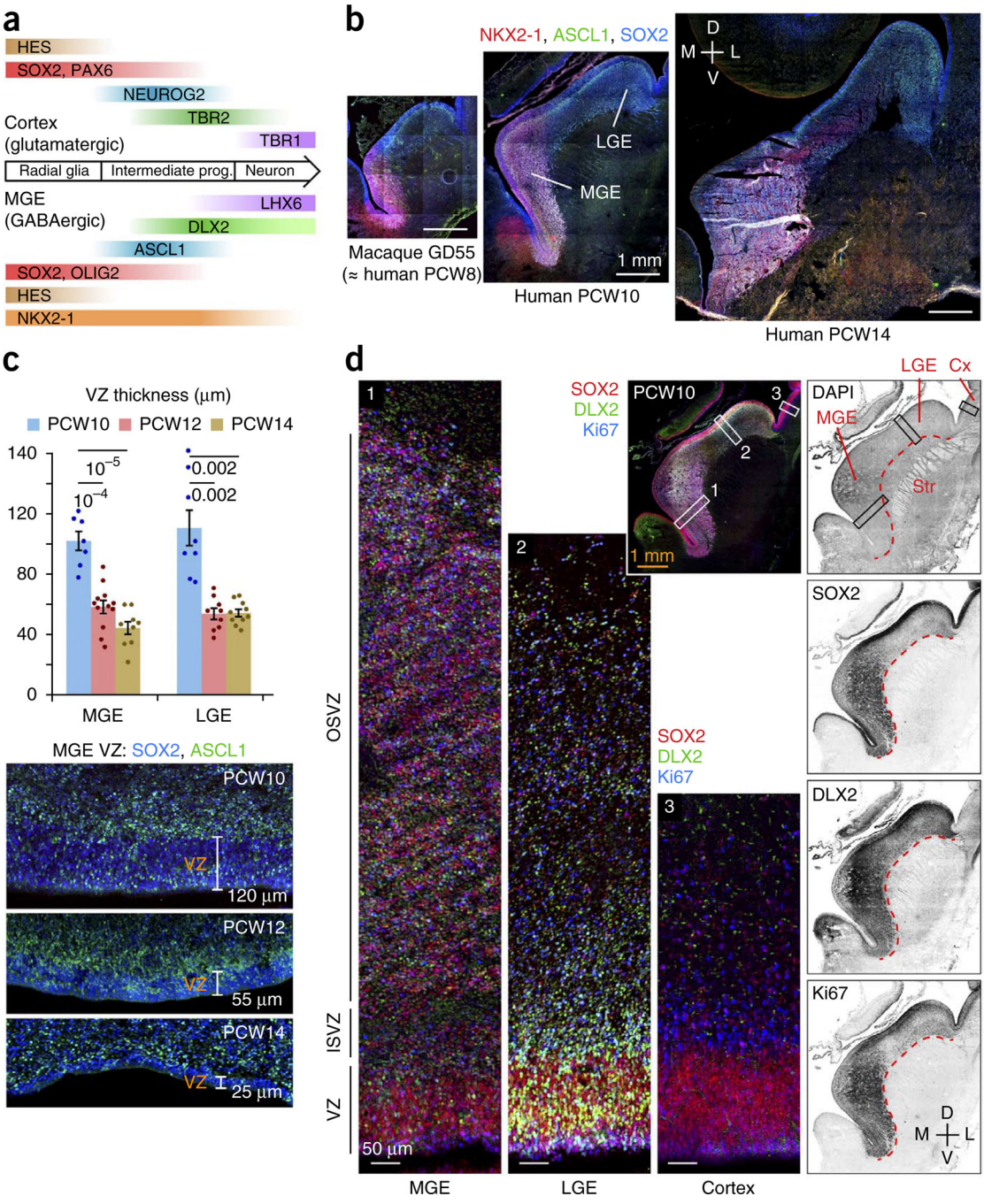


**Figure 1.**

Developmental expansion of the OSVZ in the human ganglionic eminences. (**a**) Regional transcription factors that specify neuronal subtypes also distinguish progenitor cell types. Neural stem cells in the MGE express NKX2-1 and OLIG2. In intermediate progenitor cells, ASCL1 and DLX2 repress HES and OLIG2 expression and specify differentiation into GABAergic neurons. LHX6 expression and downregulation of NKX2-1 are important for migration to the cortex. (**b**) The subventricular region of ganglionic eminence progenitor cells, marked by SOX2 and ASCL1, expanded during the early second trimester, reaching a

thickness of ~2.5 mm by PCW14 in the MGE. Macaque brain at gestational day 55 was developmentally similar to PCW8 human brain (Supplementary Fig. 1). D, dorsal; L, lateral; M, medial; V, ventral (frontal sections). (**c**) The ganglionic eminence ventricular zone (VZ) thickness diminished during the early second trimester, to as little as 25 μm in the ventromedial MGE by PCW14. Data are presented as mean ± s.e.m.; *t* test *P* values are indicated. (**d**) Comparison of germinal regions in human MGE, LGE and cortex (Cx) at PCW10 (frontal section). Outlined areas are magnified. The OSVZ in the MGE had a greater density of progenitor cells than in the LGE, and both regions exceeded the cortical OSVZ in thickness and progenitor cell density. Many $DLX2^+$ cells in the ganglionic eminences expressed Ki67, whereas cortical $DLX2^+$ cells were non-proliferative. In the medial aspect of the MGE, the weaker staining was a result of a microhemorrhage in the tissue that masked the signal. Str, striatum.

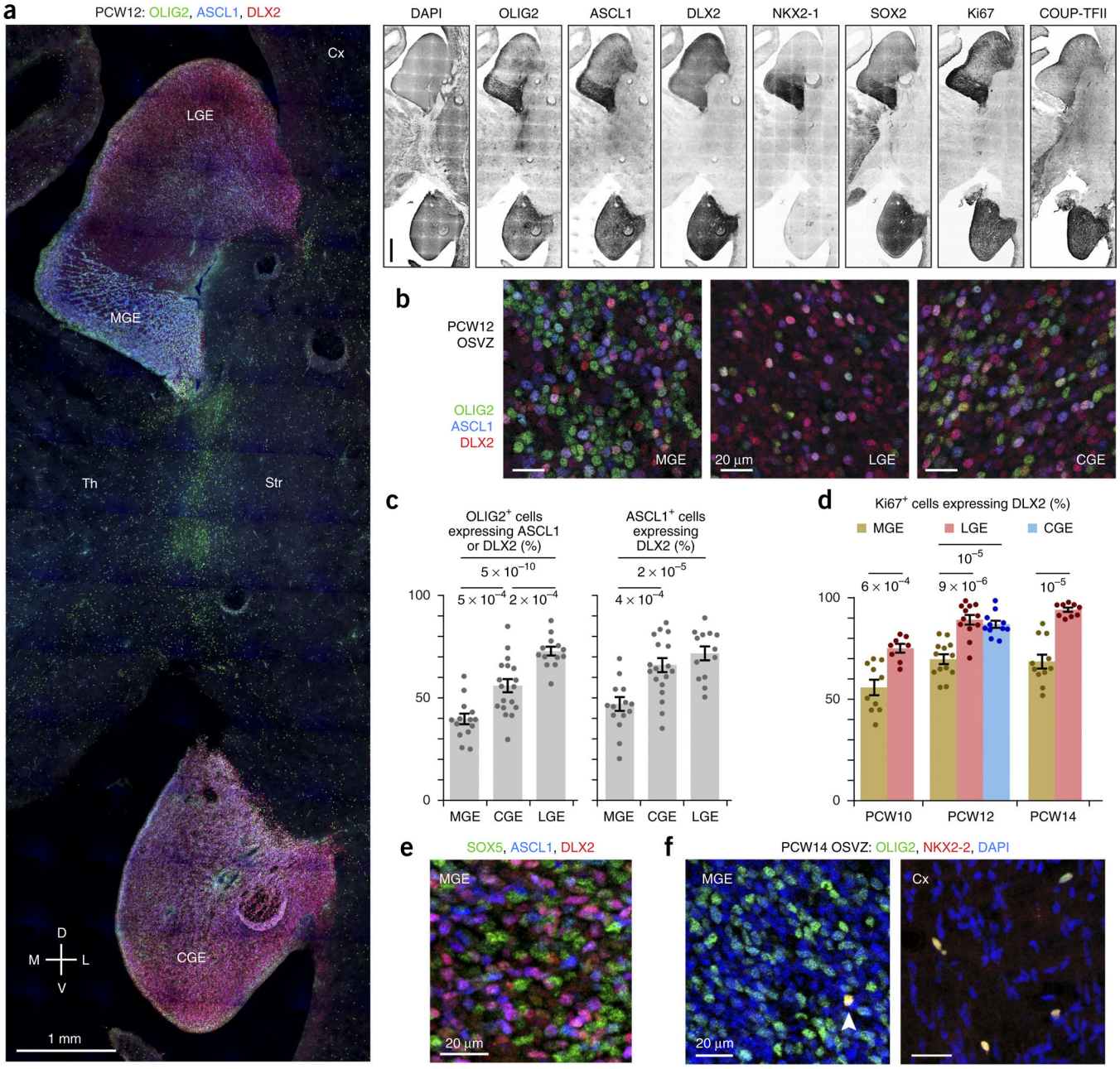


**Figure 2.**

Neural stem cells are abundant in the MGE OSVZ. (**a**) Progenitor markers of the ventral forebrain (SOX2, OLIG2, ASCL1, Ki67) labeled the human MGE (marked by NKX2-1) and CGE (marked by strong COUP-TFII) more strongly than the LGE. PCW12 frontal sections are from an intermediate location on the rostral-caudal axis. Th, thalamus. Scale bars represent 1 mm. (**b**) The MGE OSVZ had an abundance of cells expressing the same markers ($OLIG2^+$, $ASCL1^-$, $DLX2^-$) as undifferentiated radial glia in the ventricular zone. Shown are representative fields of images quantified in **c**. (**c,d**) OSVZ progenitor cells in the MGE were less differentiated than those in the CGE and LGE. $OLIG2^+$ cells were less likely to express markers of neuronal commitment, and $ASCL1^+$ and $Ki67^+$ cells were less likely

to express DLX2 in the MGE. The difference in the degree of differentiation among OLIG2$^+$ cells also reached significance when comparing CGE and LGE ($t_{29}$ = 4.37, $P$ = 0.0002). The CGE was only measured at PCW12, as it is not well developed at PCW10 and our sample of PCW14 brain tissue lacked the CGE and other caudoventral structures. Error bars represent s.e.m.; *t* test *P* values are indicated. (**e**) SOX5, expressed in radial glia of the ganglionic eminence ventricular zone, was abundantly expressed in OSVZ progenitors in the MGE. (**f**) OLIG2$^+$ cells in the human MGE OSVZ generally did not express NKX2-2, an oligodendroglial lineage marker. The arrowhead marks a rare exception. In the cortex, most or all of the sparse OLIG2$^+$ cells throughout the OSVZ and intermediate zone expressed NKX2-2.

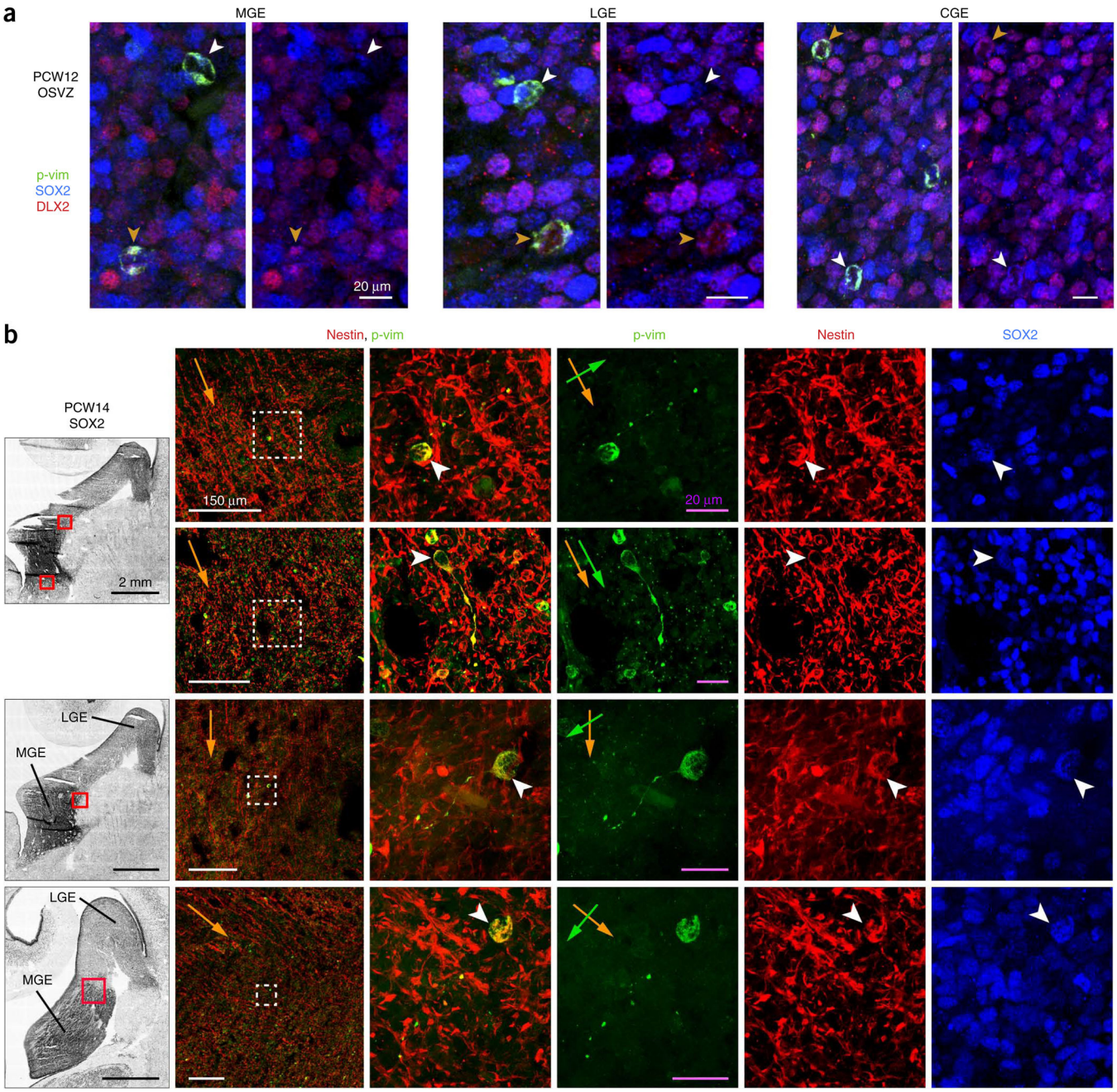


**Figure 3.**

Most OSVZ stem cells in the ganglionic eminences lack M phase fibers and are randomly oriented. (**a**) In the human ganglionic eminences, nearly all OSVZ progenitors in M phase (labeled by 4A4 antibody for p-vim) displayed a simple, rounded morphology, indicating that any glial fibers were retracted during M phase. This was true for both neural stem cells ($SOX2^+$ $DLX2^-$, white arrowheads) and intermediate progenitor cells ($DLX2^+$, orange arrowheads). (**b**) The few progenitors in the MGE OSVZ that maintained short glial fibers during M phase were unipolar, expressed SOX2 and nestin, and had random orientation. Left, SOX2 stains of ganglionic eminences in frontal PCW14 sections. Second column,

magnified images of areas boxed in red, with the overall contour of nestin fibers depicted by orange arrows. Right, magnification of the areas boxed in white showing features of $4A4^{+}$ cells that retained fibers during M phase, with cell bodies marked by white arrowheads and orientation of unipolar fibers marked by green arrows. Only one example (second row) was aligned with the overall glial fiber scaffold.

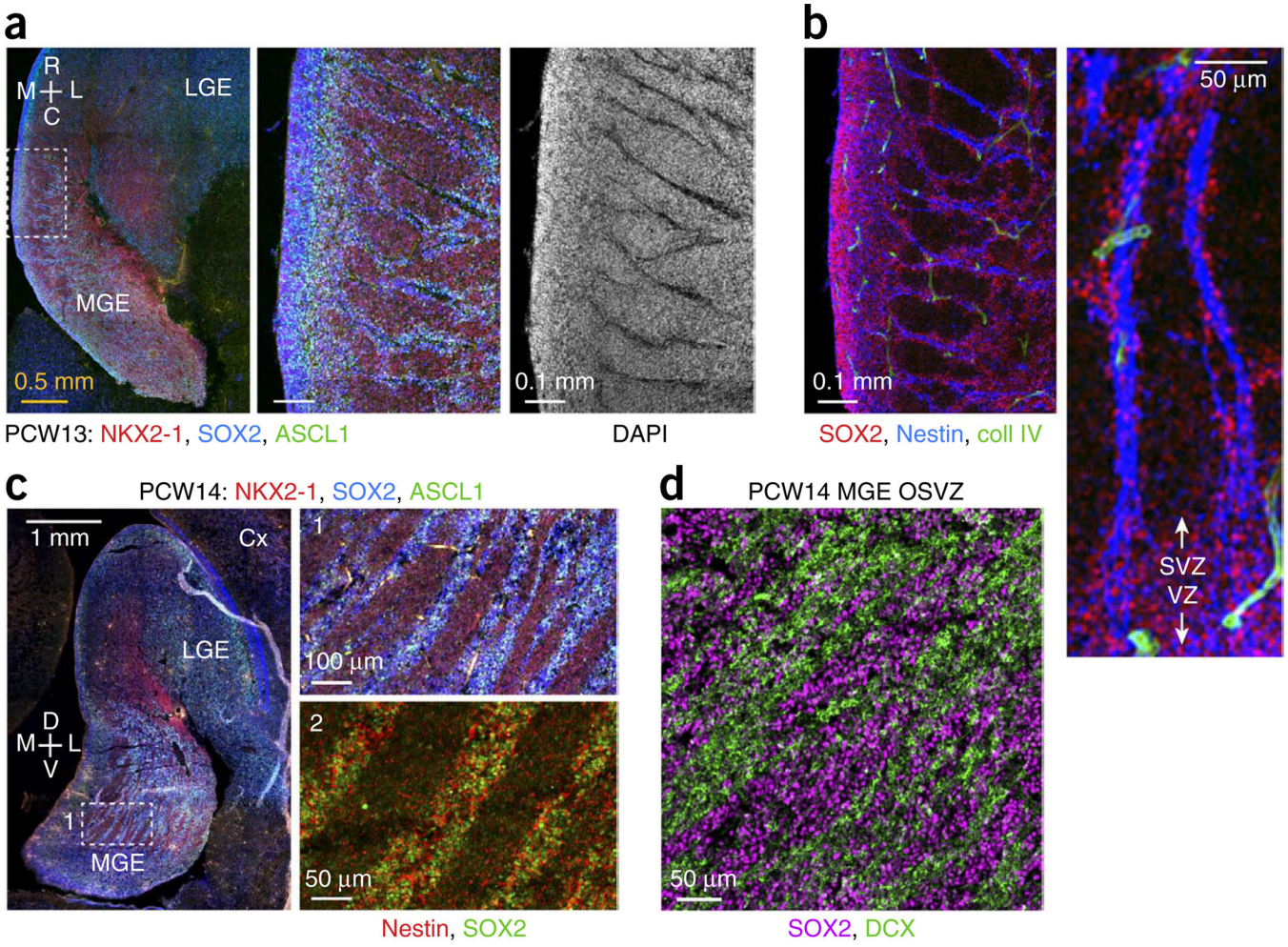


**Figure 4.**

Segregation of progenitor cells and neurons in the MGE OSVZ. (**a**) Pronounced type I clustering in PCW13 horizontal section. Magnified images of boxed area show streaks of progenitor cells that extended from ISVZ into OSVZ and were devoid of nuclei at their core ($DAPI^{-}$). C, caudal; R, rostral. (**b**) Dense bundles of radial glial fibers formed the core of type I MGE progenitor cell clusters. $SOX2^{+}$ progenitors clustered around apparent fascicles of $nestin^{+}$ fibers. The structure of the neurovasculature (marked by collagen IV) was unrelated, although points of intersection were observed. (**c**) Type II clustering of progenitor cells in PCW14 frontal sections. Left, superior ganglionic eminences from a relatively caudal location; boxed OSVZ area is magnified in panel 1. Progenitors ($SOX2^{+}$, $ASCL1^{+}$) and non-progenitor cells (NKX2-1 only) segregated into broad, elongated streaks in the MGE OSVZ, oriented toward the LGE. Nestin signal was diffusely distributed throughout type II progenitor clusters (panel 2 from an adjacent section). (**d**) Type II clusters may be formed as neurons coalesce into migratory streams out of the MGE. Cells in the $SOX2^{-}$ clusters expressed DCX, a marker of migrating neurons.

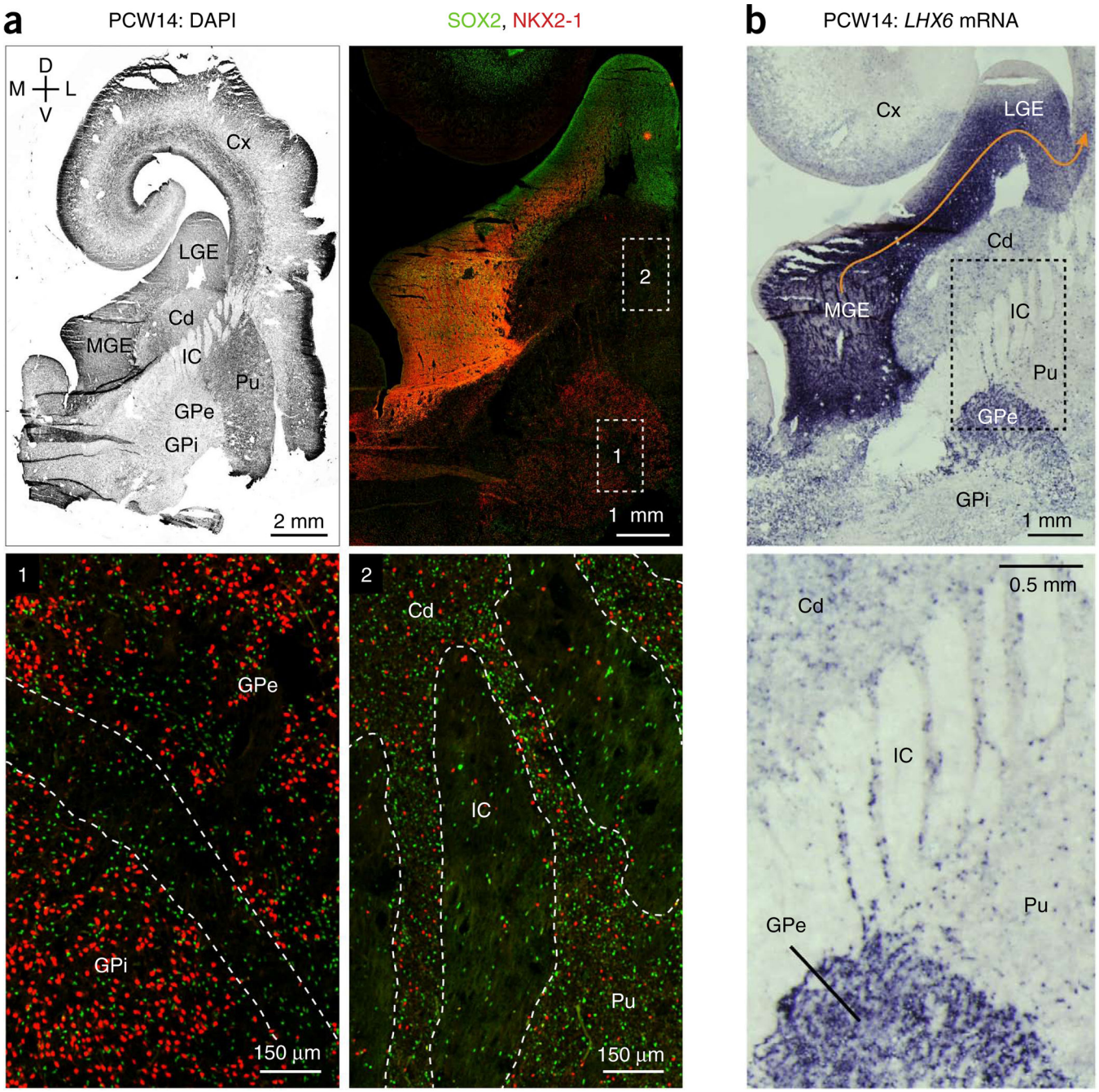


**Figure 5.**

Destinations of human MGE-derived neurons. (**a**) Distribution of NKX2-1$^{+}$ cells throughout the developing basal ganglia. Top left, PCW14 frontal section counterstained for nuclei. Ventral structures, including inferior ganglionic eminences and some cortex, were not recovered with the tissue sample. Top right, a broad view of the subpallium stained for SOX2 and NKX2-1. Note the stream of NKX2-1$^{+}$ cells with downregulated SOX2 migrating tangentially from the MGE into the LGE, toward the cortex. Boxed regions of the globus pallidus (1) and striatum (2) are magnified and shown below. The cellular bridges

that traverse the internal capsule and connect the striatal compartments are outlined (2). Cd, caudate; IC, internal capsule; Pu, putamen. (**b**) *In situ* hybridization for *LHX6* mRNA revealed sparse MGE-derived cells in the caudate and putamen, a more dense population in the GPe, and intense labeling throughout the whole LGE, the corridor for tangential migration to the cortex (orange arrow).

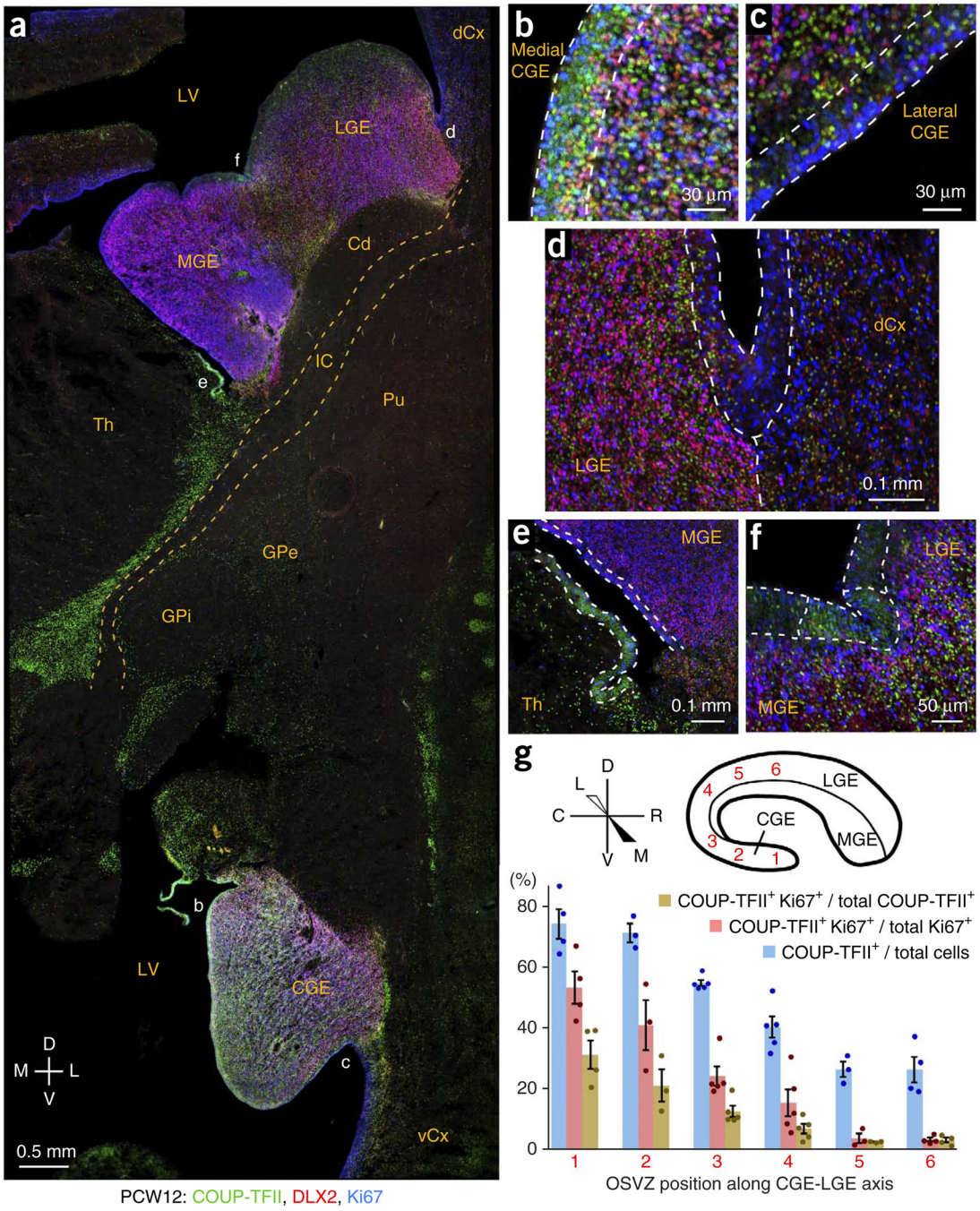


**Figure 6.**

Patterns of COUP-TFII expression in the CGE and LGE. (**a**) COUP-TFII expression was widespread in the CGE, moderate in the LGE and mostly absent in the MGE. COUP-TFII was also observed in thalamus, GPe and other brain regions. dCx, dorsal cortex; vCx, ventral cortex; LV, lateral ventricle. (**b,c**) COUP-TFII was highly expressed in the ventricular zone of medial, but not lateral, CGE. OSVZ patterning was similar, with many COUP-TFII$^{+}$ Ki67$^{+}$ cells in the medial, but not lateral, CGE OSVZ. (**d**) Coexpression of DLX2 and Ki67 in the OSVZ of LGE, but not cortex, marked the LGE-cortical boundary.

Many non-proliferating (Ki67$^{-}$) DLX2$^{+}$ cells in the LGE and cortex expressed COUP-TFII, implicating the LGE as a migratory corridor for CGE-derived cortical interneurons. (**e**) COUP-TFII was mostly absent from the MGE (except at its caudal end; Supplementary Fig. 10), but was highly expressed in the immediately ventral ventricular zone, possibly the source of a ventral stream along the thalamus' lateral edge (**a**). (**f**) COUP-TFII was expressed in a restricted region of ventricular zone (outlined) immediately surrounding the interganglionic sulcus. (**g**) COUP-TFII expression patterns indicate whether the OSVZ is more characteristic of CGE or LGE. In CGE, ~70% of OSVZ cells expressed COUP-TFII, ~30% of which were proliferating. In the LGE OSVZ, only ~25% of cells expressed COUP-TFII, almost none of which were proliferating. The transition between these extremes was gradual at intermediate points of measurement along the circumferential CGE-LGE axis. Error bars represent s.e.m.; *t* test *P* values are listed in the Source Data.

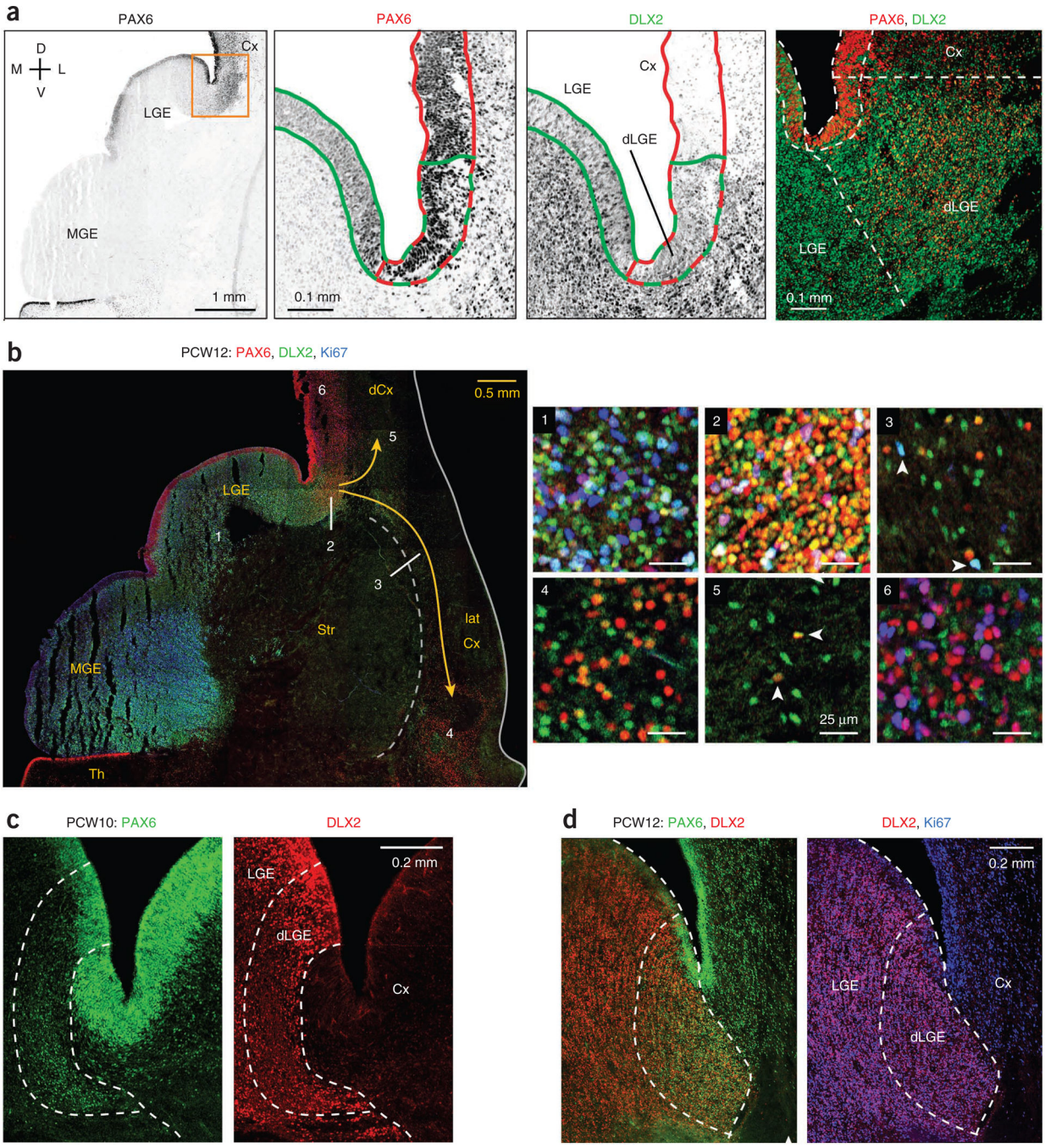


**Figure 7.**

Production of cortical interneurons in the dorsal LGE. (**a**) The LGE expressed PAX6 at low levels, except in the dLGE, where PAX6 was coexpressed at high levels with DLX2. Shown are magnified images of the boxed area of PCW12 tissue, with ventricular zone regions outlined, PAX6$^{high}$ domain in red and DLX2$^{+}$ domain in green. Right, dashed lines outlining distinct ventricular zone segments were extended into the corresponding OSVZ regions. (**b**) The dLGE supplied both the dorsal and lateral cortices with interneurons. Shown is a frontal section stained for PAX6, DLX2 and Ki67. Magnified images of the LGE

OSVZ (1), dLGE OSVZ (2), lateral cortical stream (3), lateral cortex (4), dorsal cortex intermediate zone near dLGE (5) and more distal dorsal cortex OSVZ (6) are shown. The strong PAX6 and DLX2 coexpression shown in 4 and 5 is suggestive of interneuron migration from dLGE to lateral and dorsal cortices. Arrowheads in 3 indicate proliferating migratory $DLX2^+$ cells. Arrowheads in panel 5 indicate non-proliferative $DLX2^+$ $PAX6^+$ (dLGE-derived) cortical interneurons. (**c,d**) Coexpression of DLX2 with high levels of PAX6 defined the dLGE as a progenitor cell compartment distinct from LGE or cortex. In addition, high levels of DLX2 expression indicated the dLGE-Cx boundary in ganglionic eminence progenitor cells, frequently with Ki67, whereas interneurons in the cortex expressed DLX2 at much lower levels and virtually never with Ki67. The precise location of the border between dLGE and cortex with respect to the corticostriatal sulcus varied among tissue samples.

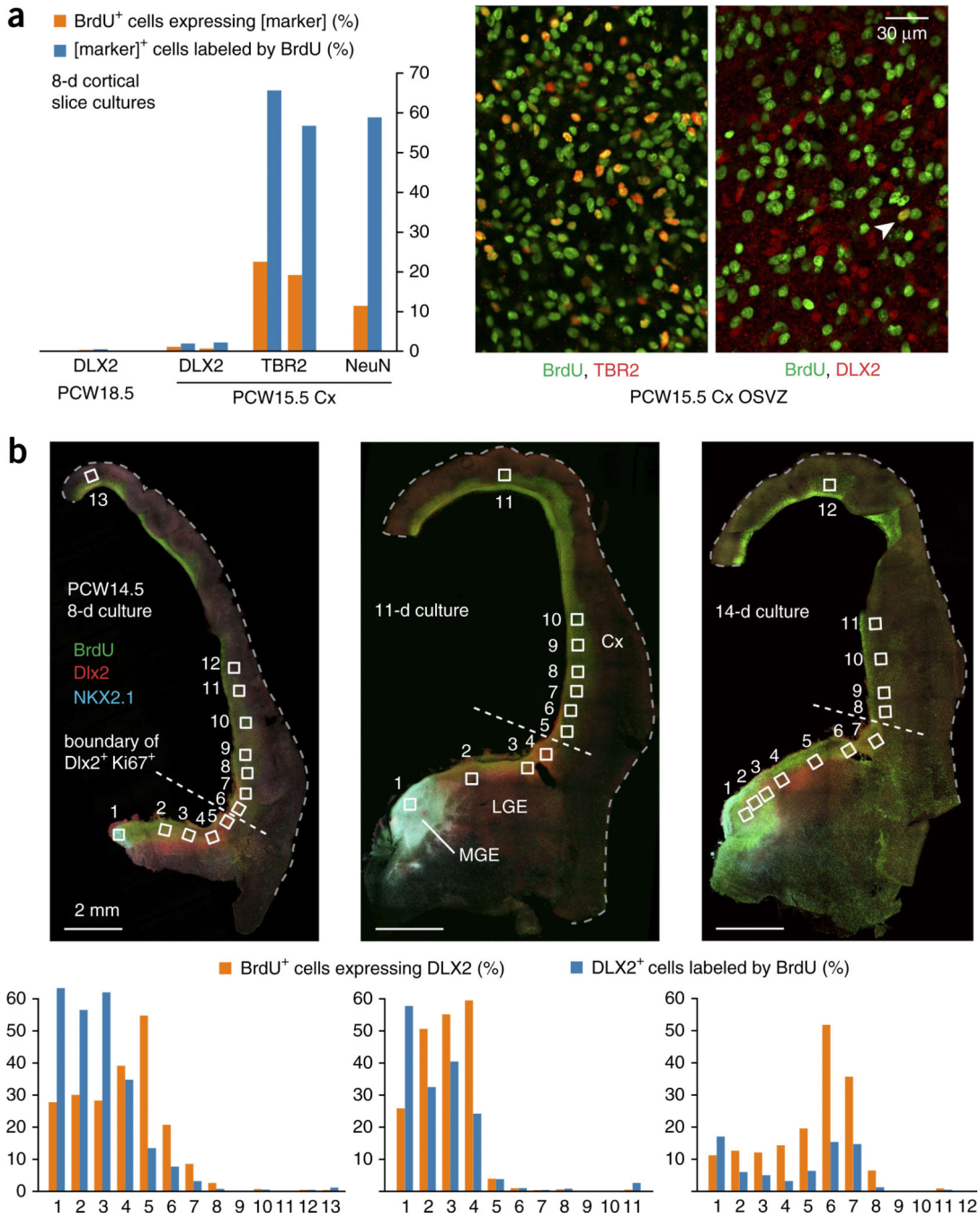


**Figure 8.**

Lack of DLX2$^+$ cell production in cortical slice cultures. (**a**) Slices of PCW18.5 and PCW15.5 cortical tissues were cultured with BrdU for 8 d and stained for BrdU and DLX2. Thousands of cells were counted and the percentage of BrdU$^+$ cells that expressed DLX2$^+$ cells was consistently less than 1%. Staining for other markers of cortical neurogenic activity revealed large numbers of BrdU$^+$ TBR2$^+$ or NeuN$^+$ cells. For DLX2 and TBR2 in slices from PCW15.5, colabeling with BrdU was measured in two different slices, with both values shown. Images show the regular colocalization of TBR2 and BrdU and an infrequent

instance of $DLX2^+$ cell production (arrowhead). (**b**) Hemispheric slice cultures including LGE/MGE from PCW14.5 were cultured with BrdU for 8–14 d. OSVZ images were captured and analyzed for DLX2 and BrdU colabeling from the numbered locations. Less than 1% of the $BrdU^+$ cells in the cortex expressed $DLX2^+$ at any time point, except in fields bordering the LGE, where we observed limited evidence of tangential migration. Additional images were taken from other locations in the cortical wall to assure that diverse regions were examined for evidence of interneuron production or migration.